

## Evolution of BSI Multi-Collection-Gate Image Sensors -From Light-in-Flight imaging to Giga-fps Continuous Imaging-

by T. Goji Etoh<sup>1)\*</sup>, Nguyen Ngo<sup>1)</sup>, Anh Quang Nguyen<sup>3)</sup>, Yoshiyuki Matsunaga<sup>1)</sup>, Taeko Ando<sup>1)</sup>,  
Kohsei Takehara<sup>2)</sup>, and Kazuhiro Shimonomura<sup>1)</sup>

<sup>1)</sup> Ritsumeikan University, <sup>2)</sup> Kindai University, <sup>3)</sup> Hanoi University of Science and Technology

\* Correspondence, [yb6t-etu@asahi-net.or.jp](mailto:yb6t-etu@asahi-net.or.jp)

### Abstract

This paper reviews evolution of the BSI MCG (Backside-Illuminated Multi-Collection-Gate) image sensors for ultra-high-speed imaging from the current status to the futuristic view. The structure originally employed a p-well for potential separation of the backside photoelectron conversion layer and the front-side circuit layer<sup>1)</sup>. The test sensor achieved the frame interval of 10 ns<sup>2)</sup>, and successfully captured flying light for the first time as a silicon image sensor<sup>3)</sup>. By replacing the p-well structure for the potential separation by a silicon light/electron guide pipe or a convex pyramid charge collector, the temporal resolution will reach 50 ps to 100 ps<sup>3)</sup>. The theoretical resolution limit is 11.1 ps as proved by Etoh, et al.<sup>4)</sup> All these image sensors work in the burst imaging mode with in-pixel signal storage. Further evolution is proposed with an additional cascade pipeline structure for the in-pixel analogue or digital storage in a stacked memory chip operating at 1 Gfps ( $\Delta t = 1$  ns), and, hopefully, for continuous readout of the processed signals.

### 1. Introduction

The theoretical highest frame rate of silicon image sensors is 11.1 ps<sup>4)</sup>. Practical image sensor structures achieving the temporal resolution of 50 ps to 100 ps have been proposed<sup>3)</sup>. The resolution of 10 ns has been achieved with a backside-illuminated multi-collection-gate image sensor<sup>2)</sup> and applied to light-in-flight imaging<sup>3)</sup>. A driver circuit to decrease the resolution to sobnanoseconds was proposed. The driver chip stacked to the sensor chip was fabricated and tested<sup>5)</sup>. This paper reviews the achievements and proposes the applications.

Advanced image sensors can detect a single photon. The pixel size is close to the diffraction limit. On the other hand, the temporal resolution of the fastest image sensor is 1,000 times the theoretical limit (10 ns/11.1 ps). High-speed is a remaining attractive research field on the image sensor.

### 2. BSI MCG Image Sensor

#### 2.1 Sensor Structure

Fig. 1 shows one pixel of the backside-illuminated multi-collection-gate image sensor with the p-well ((A) in Table 1). Signal electrons generated by incident light are collected by one of the six collection gates placed at the center. A higher voltage  $V_H$  is applied to the collection gates in turn at an interval of 10 ns. One collection gate is connected to a drain. Therefore, continuous five frames are captured at the frame interval. The pixel count is 600 kpixels. The interlace operation increases the frame count to 10 frames, sacrificing the pixel count to the half.

#### 2.2 Light-in-Flight Imaging with a Silicon Image Sensor

Fig. 2 shows a pulsed laser beam reflecting at a pair of mirrors erected with the distance of 7.43 m. The light-in-flight was

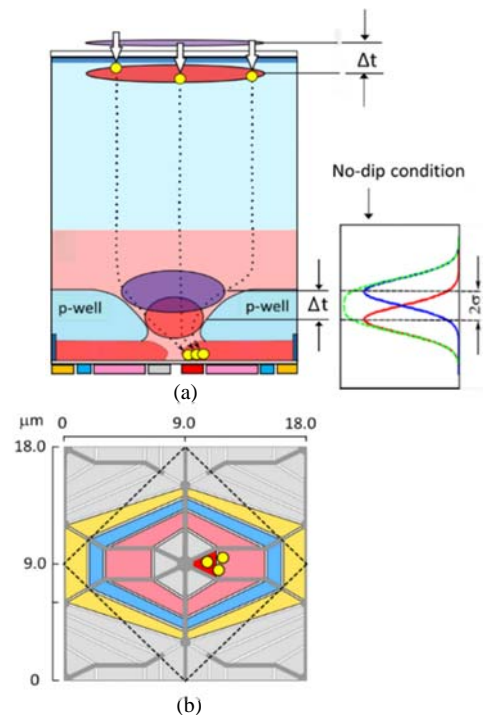


Fig. 1 A pixel of a BSI MCG image sensor<sup>1)4)</sup>

(a) A cross section, (b) A structural pixel area (a colored structure) and an optical pixel area (the dashed lines)

If  $\Delta t > 2\sigma$ , a dip appears on the superposed two Gaussian pdfs, where  $\sigma$  is the standard deviation of the arrival time. Therefore, the separation condition is expressed by  $\Delta t = 2\sigma$ .

captured by the BSI MCG image sensor for the first time as the imaging with a silicon image sensor.

### 3. Suppression of Horizontal Motion

#### 3.1 Infinitesimal Pipe and Theoretical Temporal Resolution Limit

Fig. 3 shows example trajectories of signal electrons travelling in the BSI MCG image sensor. The spread of the arriving time of the electrons is mostly caused by the horizontal motion over the p-well. If the incident light is focused at the center of the backside and the light and the generated electrons are guided through the infinitesimal silicon pipe, there is no horizontal motion. Under the assumption, a simple approximate expression of the temporal resolution limit was theoretically derived. It is 11.1 ps for silicon image sensors. Fig. 4 compares the expression with the numerical calculation results of the rigorous formulation. They almost perfectly agree.

#### 3.2 Structures for Potential Separation and Charge Collection

Table 1 compares the structures for the potential separation and the charge collection. The fill factor for the square electron/charge guide pipe (B) is 10 %. Some other conditions are adjusted for practical applications. The square pipe can be fabricated with existing technologies. However, electrons generated by X-rays outside the pipe are wasted.

A convex pyramid array charge collector (C) is also proposed. The fill factor is now 100%. It is also ideal for ultra-high-speed X-ray imaging. However, a fabrication technology for the high-quality convex silicon pyramid arrays is not available at this moment. A right-half of Fig. 5 shows the potential profile optimized for the charge collection. The temporal resolution 50 ps to 100 ps can be achieved by these technologies.

Fig. 6 shows an example of a test fabrication of a convex silicon pyramid array by Ando (the fifth author).

### 4. Cascade Pipeline MCG structure

#### 4.1 More Frame Count and Slower Operation

The number of the collection gates in a pixel is four to eight. The frame count of the MCG image sensors is limited to the number. For more collection gates, it is difficult to avoid migration of signal electrons to other gates than the collecting gate to which VH is applied.

A MCG image sensor which captures continuous 1,220 frames was developed<sup>6)</sup>. The sensor is equipped with four collection gates. A four-phase CCD with 305 elements for the signal storage is attached to each collection gate ( $1220 = 4 \times 305$ ). The four-phase CCD perfectly synchronizes with the signal collection with

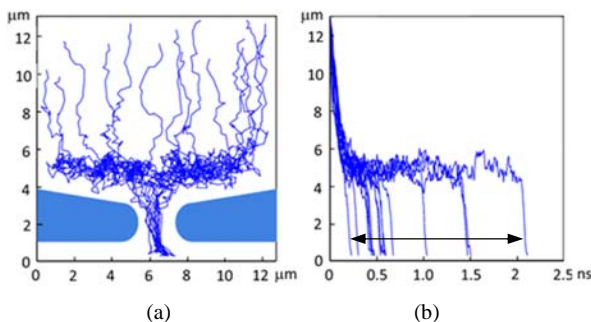


Fig. 3 Electrons' motion in the sensor shown in Fig. 1<sup>4)</sup>  
 (a) Example trajectories, (b) Arrival depths (z) from the backside vs. arrival time at the depths (x)

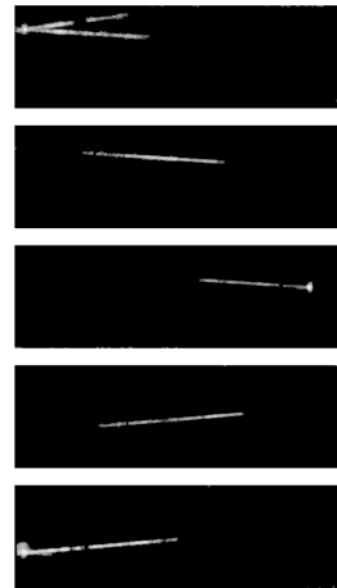


Fig. 2 Light-in-flight imaging<sup>3)</sup>  
 With the test BSI MCG image sensor. (The last 5 frames from the consecutive 10 frames.)

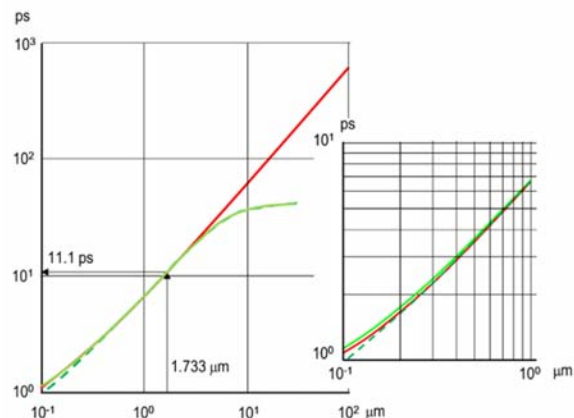


Fig. 4 Comparison of the approximate expression of the temporal resolution limit<sup>4)</sup> with the numerical calculation of the rigorous formulation<sup>3)</sup>

Green solid and dashed lines: rigorous formulation and the derived approximate expression for green light of  $\lambda = 550$  nm; red solid and dashed lines: those for 10 keV X-ray.

the four collection gates for the pipeline signal transfer. The configuration provides not only the large frame count, but also the slower operation rate of the memory CCD. The rate is one fourths of the signal collection rates thanks to the tetra-furcation with four collection gates.

#### 4.2 Multi-furcation

Multi-furcation further reduces the operation rate of the end elements. Furthermore, if the whole route from a collection gate to an end element is a buried channel, the signal electrons are completely transferred. Then, the signals are converted to voltage signals at the end elements, and transferred to a stacked memory chip at a sufficiently low rate with low noise.

Table 1 Structures for potential separation and charge collection<sup>3)</sup>  
Pixel size, 12.73  $\mu\text{m}$ ; Thickness, 13.1  $\mu\text{m}$ , Voltage amplitude to drive collection gates, 2 V; Width of the light-electron guide pipe (square), 4  $\mu\text{m}$ ; Outlet of the pyramid (square), 3  $\mu\text{m}$




Structures	A. p-well <sup>1)</sup>	B. Light/electron guide pipe <sup>2)4)</sup>	C. Convex Si pyramid <sup>3)</sup>
Cross section			
Temporal resolution: $2\sigma$	990.0 ps	49.0 ps	87.5 ps
Fill factor	100%	10%	100%
Vertical field	5 kV/cm	25 kV/cm	25 kV/cm
Collection ratio	100%	100%	98%
Dark current	less	middle	large
X-ray	Applicable	Low efficiency	Ideal
Tech. feasibility	Already applied	Existing technology	Process improvement

Fig. 7 shows an example with two-stage branching (furcation) with three buried transfer gates attached to each of six collection gates, reducing the end operation rate to 1/18 of the signal collection rate. When the image capture rate is 1 Gfps ( $\Delta t = 1 \text{ ns}$ ), the readout rate is about 50 Msps ( $\Delta t = 18 \text{ ns}$ ), which may make possible even the in-situ digital recording in the stacked digital chip, if a low dynamic range is required in the digitization.

#### 4.2 Simulations

The structure in Fig. 7 was prepared to confirm the technical feasibility and seek for the problems associated with the multi-furcation. The size of the pixel is 14  $\mu\text{m}$ . The parameters on the geometry, the concentration of the dopants and the voltages are adjusted through trial simulations. Preliminary simulation study is proceeding. The pros and cons of the structure will be presented in the conference.

### 5. Applications

#### 5.1 Time-of-Flight and Lifetime Imaging

The sub-nanosecond image sensors, together with high compatibility to computers and low noise, will innovate advanced analytical apparatuses using time-of-flight and lifetime measurements, such as imaging TOF-MS, FLIM, pulse neutron tomography, PET, LIDAR, and more, beyond these known applications.

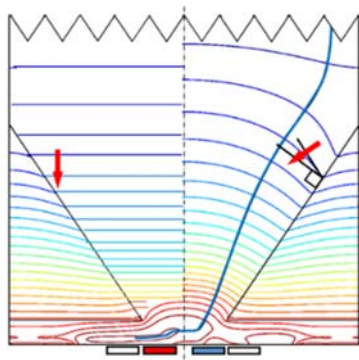


Fig. 5 A pyramid charge collector  
Right: a thin B layer on the slope and a small circular P from the front surface are implanted and optimized<sup>2)</sup>.

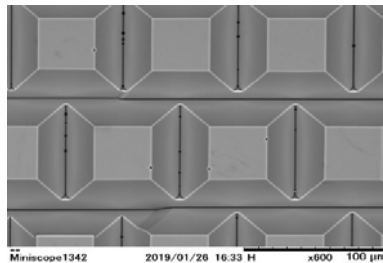


Fig. 6 An example of a fabricated convex silicon pyramid array of 80  $\mu\text{m}$   
Black dot-like defects and a slight unconfomable alignment appear.

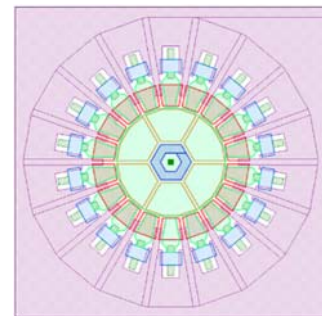


Fig. 7 An example of the cascade Pipeline MCG image sensor  
Trifurcation for each MCGs to 18 FDs reduces operation rate to 1/18.

## 5.2 Ultra-high-speed Near Infrared Image Sensor

The highest demand for high-speed video cameras in science and industrial applications lies at the frame rate at 10 kfps. For infrared high-speed imaging, there is another demand peak at around 1 Mfps, since most of imaging targets for ultra-high-speed imaging emit instant strong heat, such as in crush, explosion, ignition, and laser processing. However, the highest frame rate of existing infrared video cameras is only 10 kfps.

The electron mobility in Ge is higher than in Si. Solubility to water of GeO<sub>2</sub> has prevented use of Ge semiconductors. Recently, the demand for high speed data processing has encouraged the improvement of Ge and GeSi processes. For example, a thin Al<sub>2</sub>O<sub>3</sub> layer over the GeO<sub>2</sub> efficiently improves the chemical stability<sup>7)</sup>.

Germanium forms the diamond crystal as Silicon, which enables the fabrication of the square charge collection pipe and probably the convex pyramid charge collector array, though it's difficult to produce them due to the much smaller anisotropic etching ratio of Ge than Si. Still, a V-notch array on a Ge surface was realized as a diffraction grating already in 1996<sup>8)</sup>. Germanium is a promising candidate material for the ultra-high-speed infrared imaging.

## 5.3 Fiber-communication with Image Sensor Technology

In high-speed fiber communication, signals are detected by directly sensing photo-current generated by a very small but high-intensity laser<sup>9)</sup>. The transfer rate is more than 20 GHz ( $\Delta t = 50$  ps). On the other hand, image sensors detect a very small number of photoelectrons, based on the voltage detection of stored charge packets by the great invention of the floating diffusion with the CDS. Currently, it is possible to detect one photon if the readout rate is low. As explained above, the frame rate of ultra-high-speed image sensors will exceed 10 Gfps. It is a time to examine the possible use of technologies developed for the ultra-high-speed image sensors to the fiber communication. Germanium sensors may be the best candidate for the application, since the wave length of light for the highest transmissibility of the optical fiber is close to the wave length for the highest sensitivity of the Ge layer with several micron thick. The feasibility of the proposal should be confirmed by the following comparisons:

- (1) The power consumption of the laser for the direct current detection vs. the power consumption to drive the image sensor at more than 10 Gfps, and
- (2) The noise level vs. the operation speed at the voltage conversion in the ultra-high-speed image sensor.

## 6. Concluding Remarks

Recent achievements on ultra-high-speed image sensors by the authors are briefly reviewed. Since 1991, we have updated the highest frame rate of the image sensors in the world<sup>4)</sup>. The corresponding author is 73 years old. Therefore, his dream for the next generation ultra-high-speed image sensors is also presented in the sections 4 and 5.

This research was supported by JST A-STEP AS2526901J (Rep.: Astrodesign Inc.; Advisor: T. G. Etoh), the Grant-in-Aids for Scientific Research: (B)18H01548 (Rep.: K. Takehara), and (B)19H02204 (Rep.: K. Shimonomura), and a new technology development foundation, project No. 746 (Rep.: Astrodesign Inc.).

## References

- 1) T. G. Etoh, et al., Toward one Giga Frames per Second—Evolution of in-Situ Storage Image Sensors, *Sensors*, 13(4), 4640–4658, (2013).
- 2) A. Q. Nguyen, et al., Toward the ultimate-high-speed image sensor: from 10 ns to 50 ps, *Sensors*, 18(8), 2407 (2018).
- 3) T. G. Etoh, et al., Light-in-Flight imaging by a silicon image sensor: Toward the theoretical highest frame rate, *Sensors*, under review.
- 4) T. G. Etoh, et al., The theoretical highest frame rate of silicon image sensors, *Sensors*, 17(3), 483 (2017).
- 5) C. Zhang, et al., Pixel parallel localized driver design for a 128 x 256 pixel array 3D 1Gfps image sensor, *Proc. SPIE*, 10328-07 (2017).
- 6) V. T. S. Dao, et al., An Image Signal Accumulation Multi-Collection-Gate Image Sensor Operating at 25 Mfps with 32 × 32 Pixels and 1220 In-Pixel Frame Memory, *Sensors*, 18(9), 3112 (2018).
- 7) S. Ogawa, et al., Insights into thermal diffusion of germanium and oxygen atoms in HfO<sub>2</sub>/GeO<sub>2</sub>/Ge gate stacks and their suppressed reaction with atomically thin AlO<sub>x</sub> interlayers, *J. Appl. Phys.*, 118, 235704 (2015).
- 8) W. Lang, et al., Bulk micromachining of Ge for IR Gatings, *Journal of Micromechanics and Microengineering*, 6, 46-48 (1996).
- 9) J. Fujioka et al., High-performance MOS-capacitor-type Si optical modulator for optical interconnection, *Jpn J. Appl. Phys.*, 55, 04EC01 (2016).